Supporting Information

Regulating the hydrophobic microenvironment of SnS_2 to facilitate the interfacial CO_2/H_2O ratio towards pH-universal electrocatalytic CO_2 reduction

Zhiwei Dong [a], Yaling Jia [a, *], Zeyu Wang [a], Antony Rajendran [b], Wen-Ying Li [a, *]

[a] *State Key Laboratory of Clean and Efficient Coal Utilization, Taiyuan University of Technology, Taiyuan 030024, China*

[b] *Department of Chemistry, Mepco Schlenk Engineering College (Autonomous), Sivakasi-626005, Tamil Nadu, India.*

[*] Corresponding author.

Email address: jiayaling@tyut.edu.cn (Yaling Jia), ying@tyut.edu.cn (Wen-Ying Li)

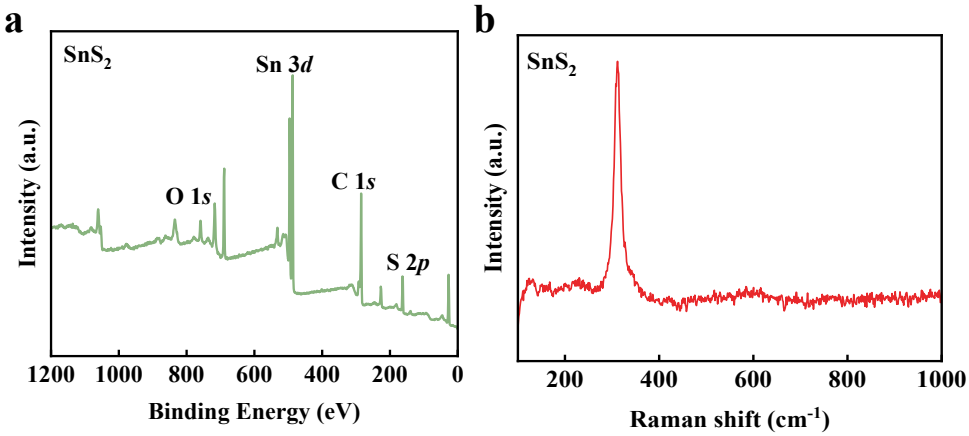

Figure S1. Characterization of SnS_2 electrodes: (a) the XPS and (b) Raman spectra of SnS_2 on CP.

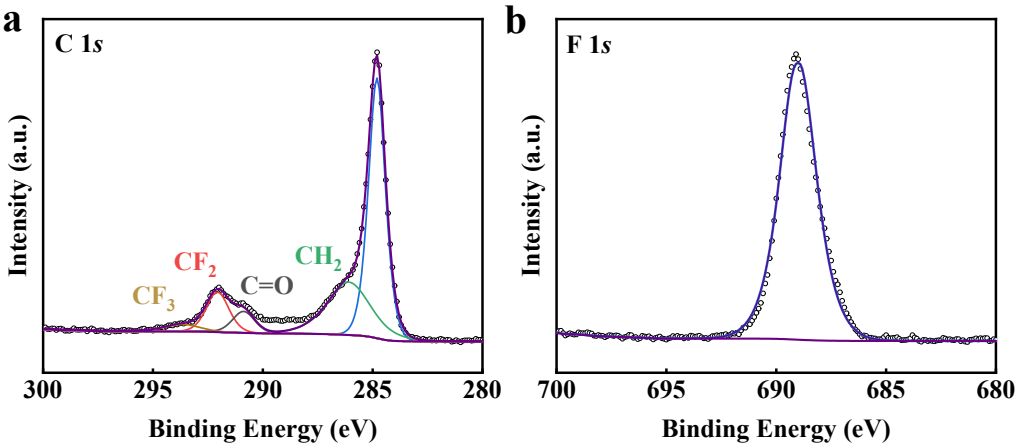

Figure S2. The high-resolution XPS spectra of (a) C 1*s* and (b) F 1*s* for SnS_2+PVDF 50.

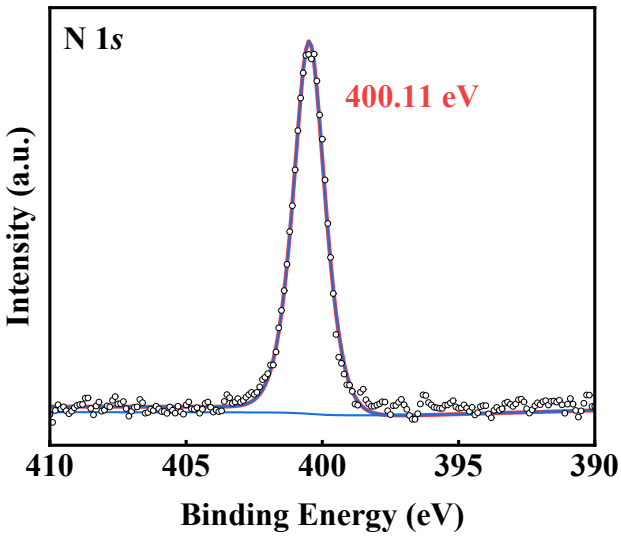

Figure S3. High-resolution N 1*s* XPS spectra of SnS_2+PVP.

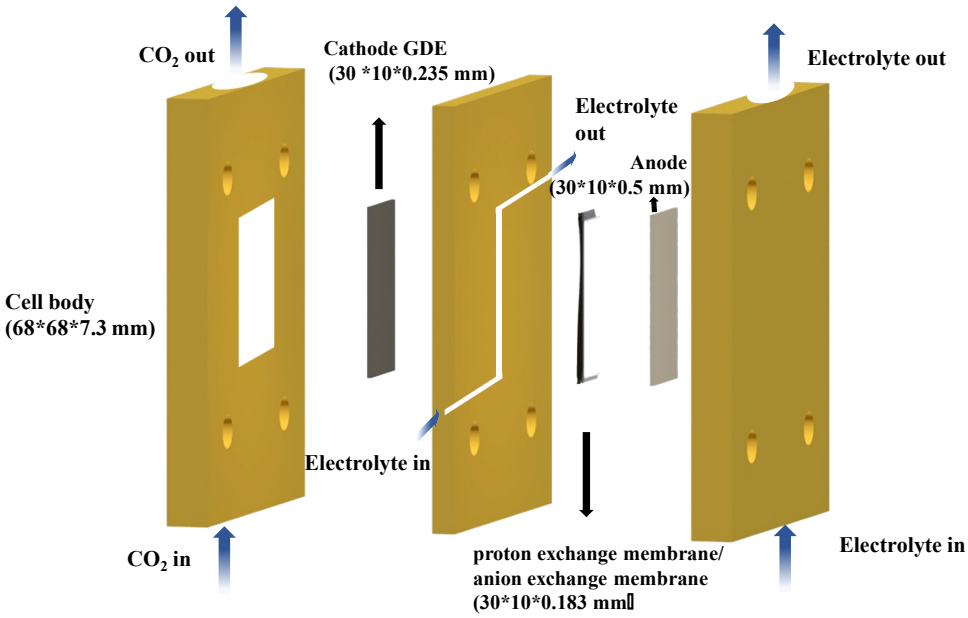

Figure S4. Schematic of the flow cell

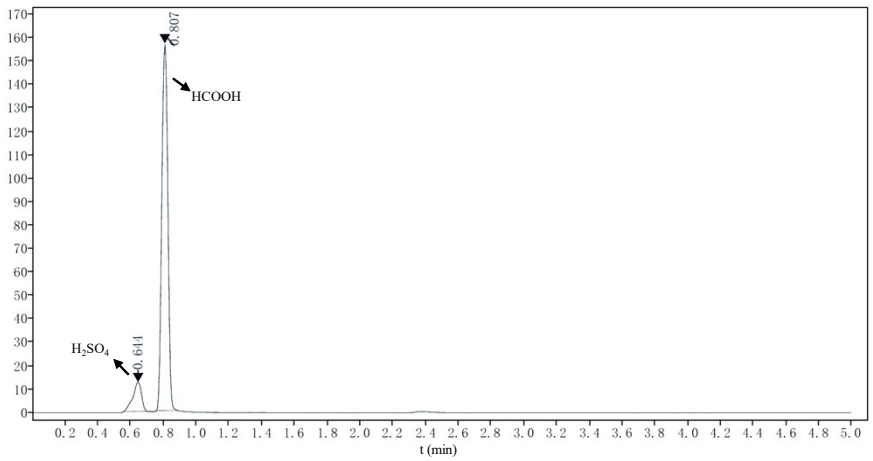

Figure S5. The result of electrocatalytic CO_2RR liquid products in HPLC

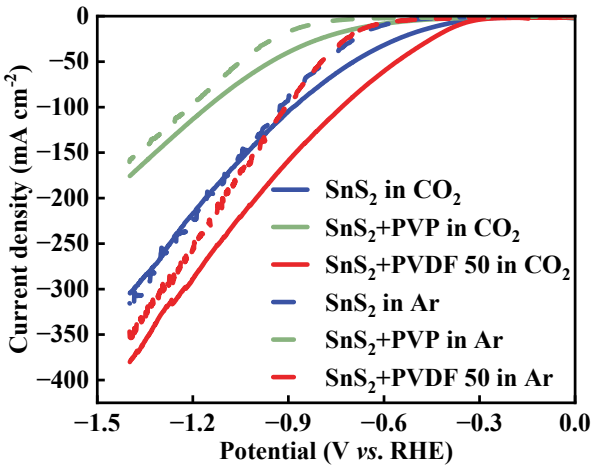

Figure S6. The LSV curves of SnS_2+PVP, SnS_2 and SnS_2+PVDF 50 electrodes in CO_2 and Ar-saturated 1.0 M KOH.

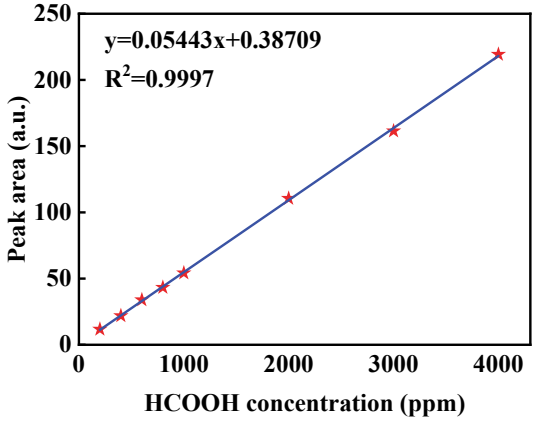

Figure S7. Formic acid standard curve obtained from HPLC.

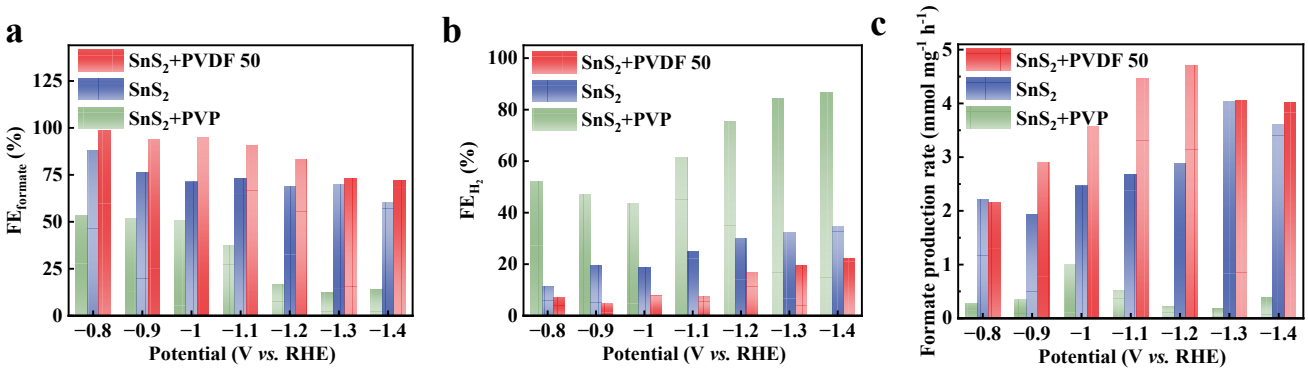

Figure S8. ECO_2RR performance comparison of (a) the formate FE, (b) the H_2 FE and (c) the formate production rate in 1 M KOH.

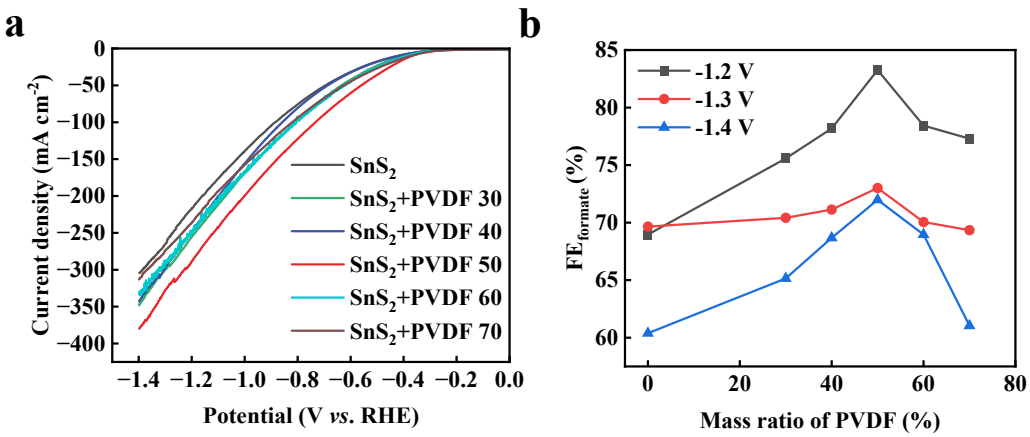

Figure S9. Evaluation of the Effect of different PVDF ratios on CO_2RR Performance: (a) the LSV curves under CO_2 and (b) FE for ECO_2RR at different potentials on SnS_2+PVDF electrodes with different mass ratios of PVDF in the catalyst layer.

To evaluate the influence of SnS_2's ratio on ECO_2RR, the mass of PVDF is varied and the correlated LSV and FE are evaluated (Figure S9). The activity and selectivity have a rise-then-fall trend with the increase of PVDF mass, reaching a maximum in SnS_2+PVDF 50.

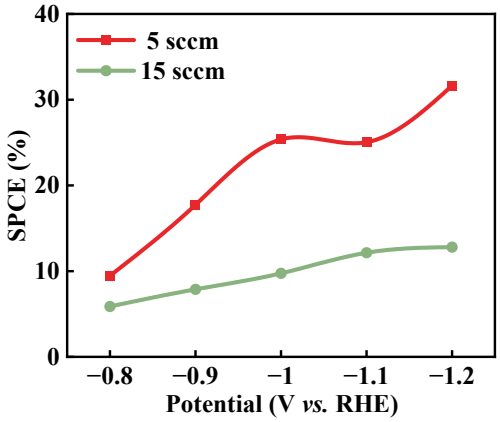

Figure S10. The variation of SPCE values under different flow rates: The SPCE of SnS_2+PVDF 50 electrode under different CO_2 flow rates (5 sccm and 15 sccm) in 1 M KOH.

The SPCE of SnS_2+PVDF 50 electrode under different CO_2 flow rates (5 sccm and 15 sccm) is compared. The SPCE value follows an increasing trend from 15 sccm to 5 sccm.

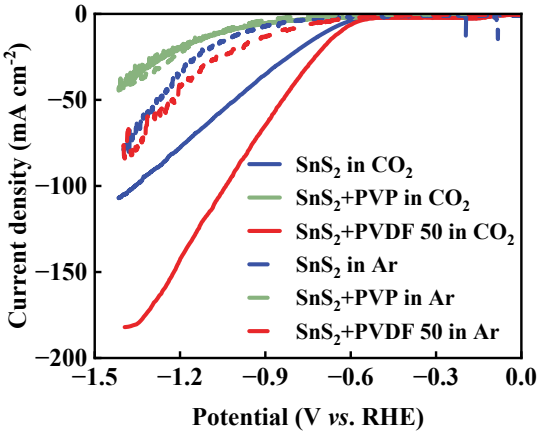

Figure S11. The LSV curves of SnS_2+PVP, SnS_2 and SnS_2+PVDF 50 electrodes in CO_2 and Ar-saturated 0.5 M $KHCO_3$.

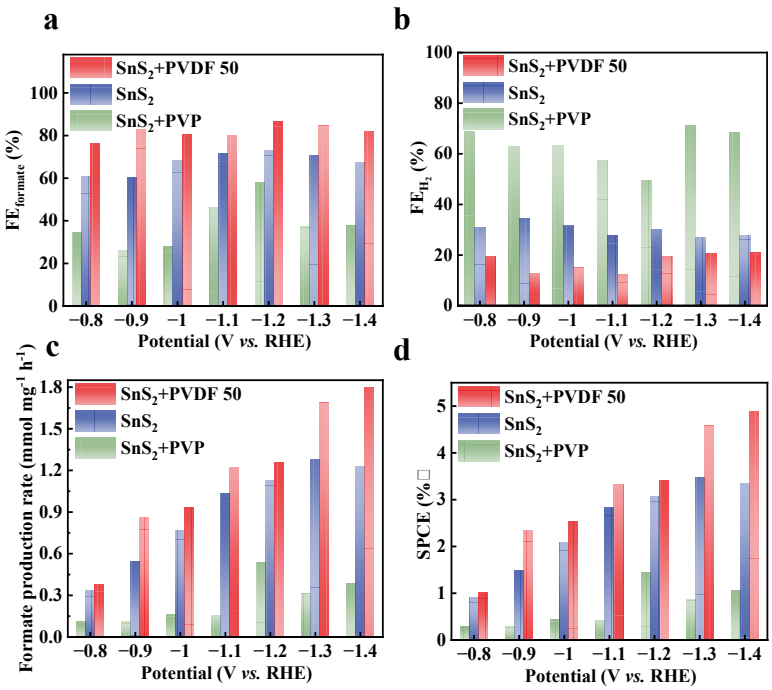

Figure S12. ECO_2RR performance comparison of (a) the formate FE, (b) the H_2 FE, (c) the formate production rate, and (d) the SPCE of SnS_2+PVDF 50, SnS_2 and SnS_2+PVP in 0.5 M $KHCO_3$.

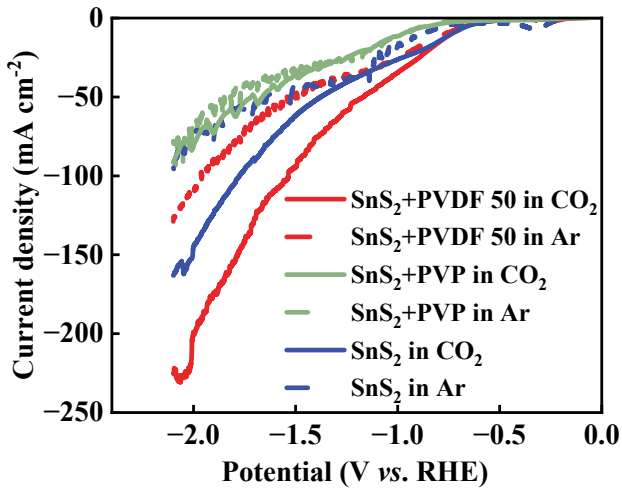

Figure S13. The LSV curves of SnS_2+PVP, SnS_2 and SnS_2+PVDF 50 electrodes in CO_2 and Ar-saturated 0.05 M H_2SO_4+0.5 M K_2SO_4.

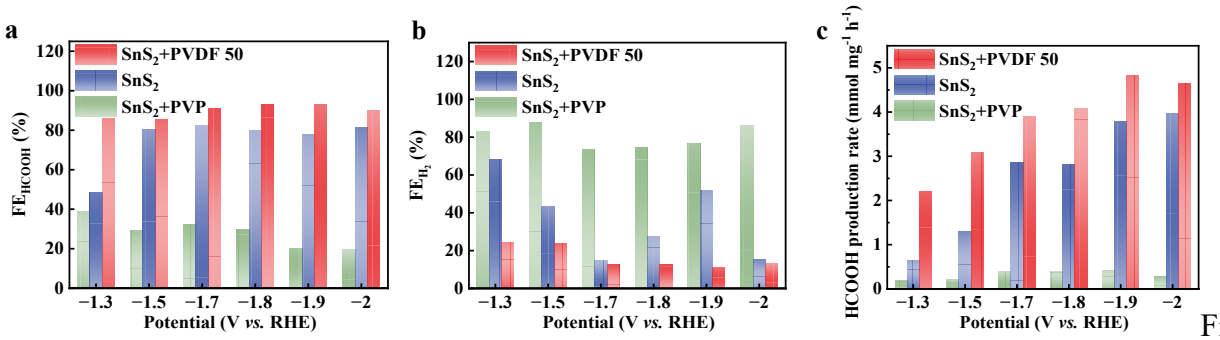

Figure S14. ECO_2RR performance comparison of (a) the HCOOH FE, (b) the H_2 FE, (c) the HCOOH production rate of SnS_2+PVP, SnS_2 and SnS_2+PVDF 50 electrodes and SnS_2+PVP in 0.05 M H_2SO_4+0.5 M K_2SO_4.

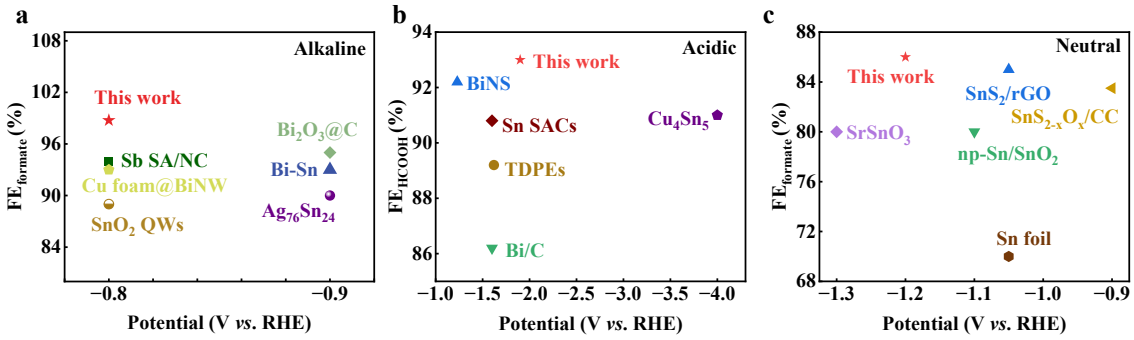

Figure S15. The comparison of HCOOH FE in pH universal electrolytes.[1-16]

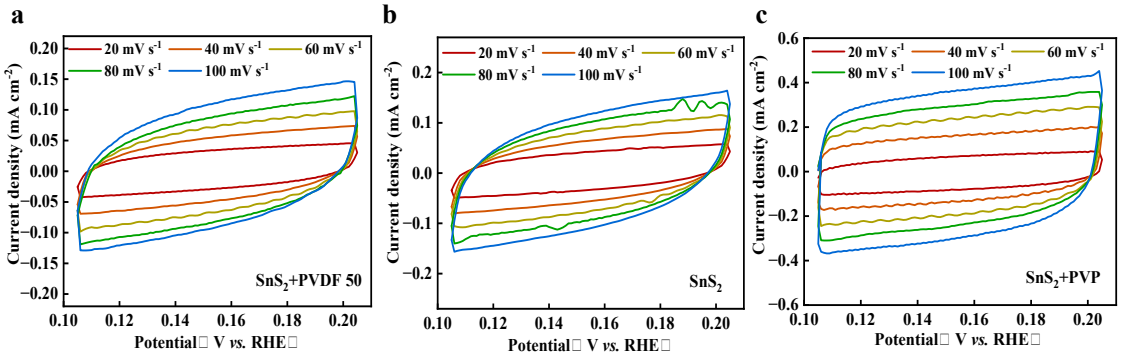

Figure S16. CV curves at different scan rates of 20 ~ 100 mV s^{-1} for (a) SnS_2+PVDF 50, (b) SnS_2, and (c) SnS_2+PVP.

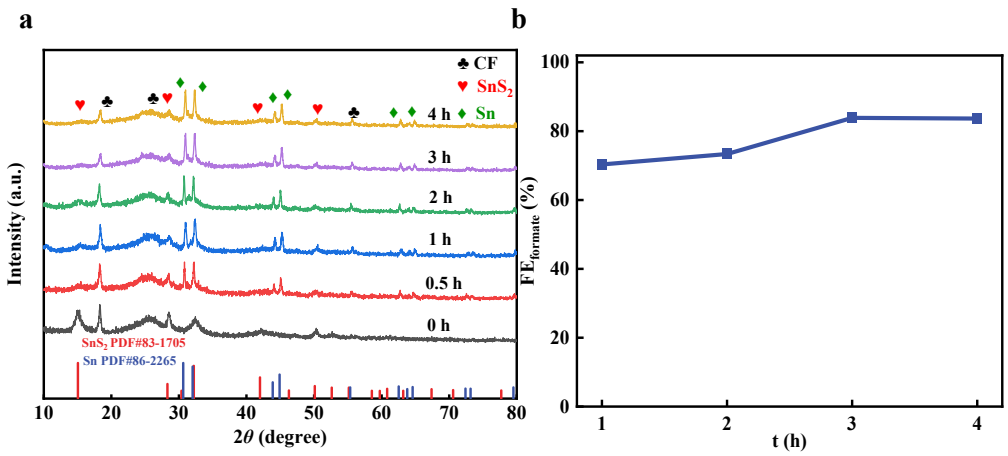

Figure S17. The change of structure and performance during CO_2RR: (a) The XRD patterns of the evolution process from SnS_2 to Sn/SnS_2 with different electroreduction treatment periods; (b) the formate FE of the SnS_2+PVDF 50 during the evolution process.

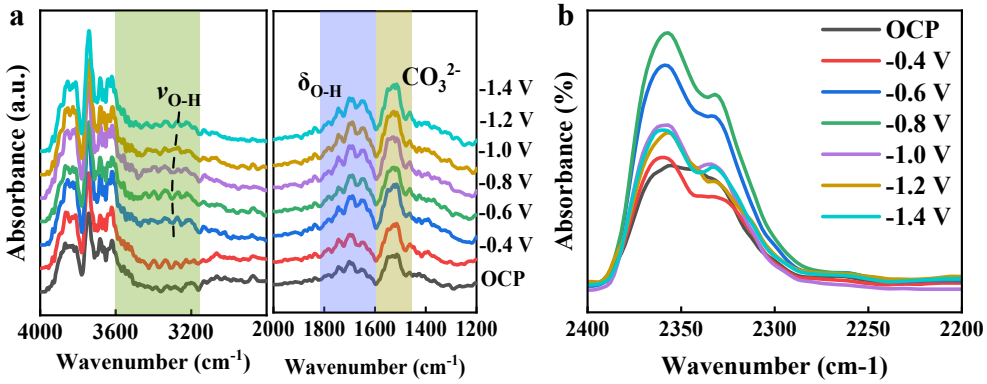

Figure S18. *In-situ* ATR-SEIRAS spectra recorded of SnS_2 in a range of different wavelength segments (a) 4000-3000 cm^{-1} and 2000-1200 cm^{-1}; (b) 2200-2400 cm^{-1}.

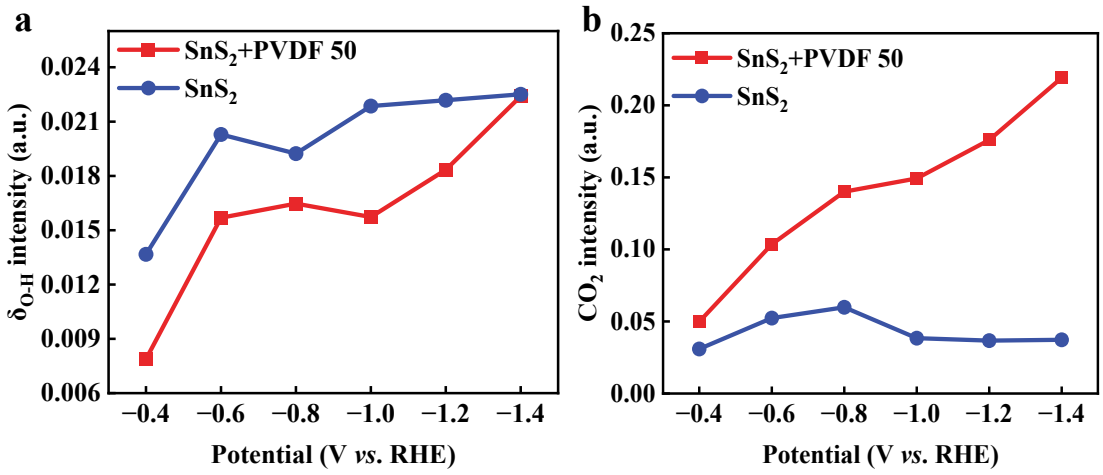

Figure S19. (a) $\delta_{O\text{-}H}$ intensity and (b) CO_2 intensity at different applied potentials from in-situ ATR-SEIRAS spectra.

Through comparison of $\delta_{O\text{-}H}$ intensity and CO_2 intensity at different applied potentials In ATR-SEIRAS spectra, it is clearly shown that the SnS_2+PVDF 50 electrode has a lower intensity of $\delta_{O\text{-}H}$ and a higher intensity of CO_2. This effectively demonstrates that PVDF creates a hydrophobic microenvironment.

Table S1. Comparisons of CO_2RR-to-formate SPCE of some advanced catalysts.

pH	Materials	Electrolytes	$SPCE_{max}$	Ref
2	BiS-1	0.05 M H_2SO_4+0.5 M K_2SO_4	65.4%	[16]
1.2	Bi-MOF-TS	0.1 M K_2SO_4 + 0.02 M H_2SO_4	62%	[17]
14	Nafion/PTFE/SnO$_2$ TPB	1 M KOH	29.3%	[18]
14	BiOON-PTFE	1 M KOH	38%	[19]
14	Bi_2O_3 nanoparticles	1 M KOH	7.2%	[5]
	Bi nanoparticles	solid electrolyte	29.1%	[20]
14	Sn_3O_4 nanosheets	1 M KOH	32.4%	[21]
14	InP quantum dots	3 M KOH	13%	[22]
1.44	SnS_2+PVDF 50	0.05 M H_2SO_4 + 0.5 M K_2SO_4	72.77%	This work

Table S2. Comparisons of CO_2RR-to-formate performances of Sn-based catalysts in acidic electrolyte.

pH	Materials	Electrolytes	Potentials (V vs. RHE)	FE_{HCOOH} (%)	Ref.
1	Cu_6Sn_5	3M KCl, 0.05 M H_2SO_4,	−4	91%	[7]
3.4	SnO	0.5 M K_2SO_4		88.4	[23]
1.67	NU-1000-Sn	0.005 M H_2SO_4 and 3 M KCl	−1.8	95	[24]
3.77	SP SnO/SnO_2 NP	0.5 M K_2SO_4		~100	[23]
1.5	SnO_2/C	0.1 M H_2SO_4 0.4 M K_2SO_4	–1.4	88	[25]
3	Sn(S)-H	0.5 M K_2SO_4, H_2SO_4	–1.5	92.15	[26]
3	Sn-SAC	0.5 M K_2SO_4, H_2SO_4		90.8	[11]
1	SnBi	0.05 M H2SO4, 3 M KCl	–1.5	95	[27]
1.44	SnS_2+PVDF 50	0.05 M H_2SO4 + 0.1 M K_2SO_4	–1.9	93	This work

Table S3. Comparisons of CO_2RR-to-formate performances of Sn-based catalysts in neutral and alkaline electrolytes.

Materials	Electrolytes	Potentials (V vs. RHE)	FE_{HCOOH} (%)	Ref.
SnOx/Sn	0.1 M $KHCO_3$	–1.05	70	[12]
SnS_2-derived Sn/rGO	0.5 M $KHCO_3$	–1.05	85	[13]
Ni doped SnS_2	0.1 M $KHCO_3$	–0.9	93	[28]
np-Sn/SnO_2	0.5 M $KHCO_3$	–1.1	80	[14]
$SrSnO_3$ NWs	$NaHCO_3$	–1.3	80	[15]
Sn-Bi/SnO_2	1 M KOH	–0.62	95	[29]
Cu-SnO_2	1 M KOH	–0.9	90	[30]
CeOx-Sn	1 M KOH	–1.07	95	[31]
Zn/SnO_2	1 M KOH	–0.9	93.2	[32]
SnS_2+PVDF 50	0.5 M $KHCO_3$	–1.2	86	This work
SnS_2+PVDF 50	1 M KOH	–0.8	98	This work

Table S4. Comparisons of CO_2RR-to-formate performances of SnS_2-based catalysts.

Materials	Electrolytes	Potentials (V vs. RHE)	FE_{HCOOH} (%)	Ref.
1T/1H-SnS_2	0.1 M $KHCO_3$	–1.31	63.4	[33]
SnS_2-derived Sn/rGO	0.5 M $KHCO_3$	–1.05	85	[13]
Ni doped SnS_2	0.1 M $KHCO_3$	–0.9	93	[28]
S-CuSn	0.5 M $KHCO_3$	–2.22	96.4	[34]
Cu_1/SnS_2	2 M KOH	–1	90.9	[35]
Sn(S)-H	0.5 M K_2SO_4, H_2SO_4	–1.5	92.2	[26]
E-SnS_2	1 M KOH	–0.84	90	[36]
$SnS_{2-x}O_x$/CC	0.5 M $KHCO_3$	–0.9	83.5	[16]
In-O-ultrathin-SnS_2	0.5 M $KHCO_3$	–1.2	88.6	[37]
SnS_2+PVDF 50	0.5 M $KHCO_3$	–1.2	86	This work
SnS_2+PVDF 50	1 M KOH	–0.8	98	This work
SnS_2+PVDF 50	0.05 M H_2SO4+0.1 M K_2SO_4	–1.5	93	This work

References:

1. Z. Jiang, T. Wang, J. Pei, H. Shang, D. Zhou, H. Li, J. Dong, Y. Wang, R. Cao, Z. Zhuang, W. Chen, D. Wang, J. Zhang and Y. Li, *Energy Environ. Sci.*, 2020, **13**, 2856-2863.
2. W. Luc, C. Collins, S. Wang, H. Xin, K. He, Y. Kang and F. Jiao, *J. Am. Chem. Soc.*, 2017, **139**, 1885-1893.
3. X. Zhang, X. Sun, S.-X. Guo, A. M. Bond and J. Zhang, *Energy Environ. Sci.*, 2019, **12**, 1334-1340.
4. S. Liu, J. Xiao, X. F. Lu, J. Wang, X. Wang and X. W. Lou, *Angew. Chem. Int. Ed.*, 2019, **58**, 8499-8503.
5. P. Deng, F. Yang, Z. Wang, S. Chen, Y. Zhou, S. Zaman and B. Y. Xia, *Angewandte Chemie International Edition*, 2020, **59**, 10807-10813.
6. Z. Wu, H. Wu, W. Cai, Z. Wen, B. Jia, L. Wang, W. Jin and T. Ma, *Angew. Chem. Int. Ed.*, 2021, **60**, 12554-12559.
7. X. Yu, Y. Xu, L. Li, M. Zhang, W. Qin, F. Che and M. Zhong, *Nat. Commun.*, 2024, **15**, 1711.
8. Y. Qiao, W. Lai, K. Huang, T. Yu, Q. Wang, L. Gao, Z. Yang, Z. Ma, T. Sun, M. Liu, C. Lian and H. Huang, *ACS Catal.*, 2022, **12**, 2357-2364.
9. T. Yan, H. Pan, Z. Liu and P. Kang, *Small.*, 2023, **19**, 2207650.
10. T. Dong, H. Li, Z. Wang, Y. Geng, R. Chang, X. Tian, J. Lai, S. Feng and L. Wang, *Nano Res.*, 2024, **17**, 5817-5825.
11. B. Sun, Z. Li, D. Xiao, H. Liu, K. Song, Z. Wang, Y. Liu, Z. Zheng, P. Wang, Y. Dai, B. Huang, A. Thomas and H. Cheng, *Angew. Chem. Int. Ed.*, 2024, **63**, e202318874.
12. J. E. Pander, III, M. F. Baruch and A. B. Bocarsly, *ACS Catal.*, 2016, **6**, 7824-7833.
13. F. Li, L. Chen, M. Xue, T. Williams, Y. Zhang, D. R. MacFarlane and J. Zhang, *Nano Energy.*, 2017, **31**, 270-277.
14. S. Liu, F. Pang, Q. Zhang, R. Guo, Z. Wang, Y. Wang, W. Zhang and J. Ou, *Appl. Mater. Today.*, 2018, **13**, 135-143.
15. Y. Pi, J. Guo, Q. Shao and X. Huang, *Nano Energy.*, 2019, **62**, 861-868.
16. T. Chen, T. Liu, T. Ding, B. Pang, L. Wang, X. Liu, X. Shen, S. Wang, D. Wu, D. Liu, L. Cao, Q. Luo, W. Zhang, W. Zhu and T. Yao, *Nano-Micro Lett.*, 2021, **13**, 189.
17. X. Chen, R. Lu, C. Li, W. Luo, R. Yu, J. Zhu, L. Lv, Y. Dai, S. Gong, Y. Zhou, W. Xiong, J. Wu, H. Cai, X. Wu, Z. Deng, B. Xing, L. Su, F. Wang, F. Chao, W. Chen, C. Xia, Z. Wang and L. Mai, *Nature Communications*, 2025, **16**, 1927.
18. H. Liu, Y. Su, Z. Liu, H. Chuai, S. Zhang and X. Ma, *Nano Energy.*, 2023, **105**, 108031.
19. Z. Xing, X. Hu and X. Feng, *ACS Energy Lett.*, 2021, **6**, 1694-1702.
20. L. Fan, C. Xia, P. Zhu, Y. Lu and H. Wang, *Nat. Commun.*, 2020, **11**, 3633.
21. L.-X. Liu, Y. Zhou, Y.-C. Chang, J.-R. Zhang, L.-P. Jiang, W. Zhu and Y. Lin, *Nano Energy.*, 2020, **77**, 105296.
22. I. Grigioni, L. K. Sagar, Y. C. Li, G. Lee, Y. Yan, K. Bertens, R. K. Miao, X. Wang, J. Abed, D. H. Won, F. P. García de Arquer, A. H. Ip, D. Sinton and E. H. Sargent, *ACS Energy Lett.*, 2021, **6**, 79-84.
23. M. Oßkopp, A. Löwe, C. M. S. Lobo, S. Baranyai, T. Khoza, M. Auinger and E. Klemm, *J. CO2 Util.*, 2022, **56**, 101823.
24. H. Xue, Z.-H. Zhao, P.-Q. Liao and X.-M. Chen, *J. Am. Chem. Soc.*, 2023, **145**, 16978-16982.
25. J. Gu, S. Liu, W. Ni, W. Ren, S. Haussener and X. Hu, *Nat Catal.*, 2022, **5**, 268-276.
26. Z. Ma, Z. Yang, W. Lai, Q. Wang, Y. Qiao, H. Tao, C. Lian, M. Liu, C. Ma, A. Pan and H.

Huang, *Nat Commun.*, 2022, **13**, 7596.
27. L. Li, Z. Liu, X. Yu and M. Zhong, *Angew. Chem. Int. Ed.*, 2023, **62**, e202300226.
28. A. Zhang, R. He, H. Li, Y. Chen, T. Kong, K. Li, H. Ju, J. Zhu, W. Zhu and J. Zeng, *Angew. Chem. Int. Ed.*, 2018, **57**, 10954-10958.
29. L. Li, A. Ozden, S. Guo, F. P. García de Arquer, C. Wang, M. Zhang, J. Zhang, H. Jiang, W. Wang, H. Dong, D. Sinton, E. H. Sargent and M. Zhong, *Nat Commun.*, 2021, **12**, 5223.
30. B. Li, J. Chen, L. Wang, D. Xia, S. Mao, L. Xi, S. Ying, H. Zhang and Y. Wang, *Appl. Catal. B Environ.*, 2025, **363**, 124784.
31. Y. Zhu, X. Sun, R. Zhang, X. Feng and Y. Zhu, *Small.*, 2024, **20**, 2400191.
32. X. Hu, G. Mei, X. Chen, J. Liu, B. Y. Xia and B. You, *Angew. Chem. Int. Ed.*, 2023, **62**, e202304050.
33. Y. Kawabe, Y. Ito, Y. Hori, S. Kukunuri, F. Shiokawa, T. Nishiuchi, S. Jeong, K. Katagiri, Z. Xi, Z. Li, Y. Shigeta and Y. Takahashi, *ACS Nano.*, 2023, **17**, 11318-11326.
34. K. Li, J. Xu, T. Zheng, Y. Yuan, S. Liu, C. Shen, T. Jiang, J. Sun, Z. Liu, Y. Xu, M. Chuai, C. Xia and W. Chen, *ACS Catal.*, 2022, **12**, 9922-9932.
35. R. Chen, J. Zhao, X. Zhang, Q. Zhao, Y. Li, Y. Cui, M. Zhong, J. Wang, X. Li, Y. Huang and B. Liu, *J. Am. Chem. Soc.*, 2024, **146**, 24368-24376.
36. Z. Liu, C. Liu, J. Zhang, S. Mao, X. Liang, H. Hu and X. Huang, *Appl. Catal. B Environ.*, 2024, **341**, 123274.
37. X. Zhang, M. Jiao, Z. Chen, X. Ma, Z. Wang, N. Wang, X. Zhang and L. Liu, *Chem. Eng. J.*, 2022, **429**, 132145.